OFFICE OF NAVAL RESEARCH

GRANT or CONTRACT N00014-90-J-1161

R & T Code 4133030

Technical Report No. 014

Characterization of Small Noble Metal Electrodes by Voltammetry and Energy Dispersive X-Ray Analysis

by

Timothy G. Strein, Andrew G. Ewing

Prepared for Publication

in

Analytical Chemistry

Department of Chemistry
Penn State University
University Park, PA 16802

January 26, 1993

REPORT DOCUMENTATION PAGE

Form Approved
OMB No 0704-0188

1. AGENCY USE ONLY (Leave blank)	2. REPORT DATE	3. REPORT TYPE AND DATES COVERED
	January 26, 1993	Technical

4. TITLE AND SUBTITLE

Characterization of Small Noble Metal Electrodes by Voltammetry and Energy Dispersive X-Ray Analysis

5. FUNDING NUMBERS

N00014-90-J-1161

6. AUTHOR(S)

Timothy G. Strein, Andrew G. Ewing

7. PERFORMING ORGANIZATION NAME(S) AND ADDRESS(ES)

Department of Chemistry
Penn State University
University Park, PA 16802

8. PERFORMING ORGANIZATION REPORT NUMBER

No: 014

9. SPONSORING MONITORING AGENCY NAME(S) AND ADDRESS(ES)

Office of Naval Research
800 N. Quincy
Arlington, VA 22217-5000

10. SPONSORING MONITORING AGENCY REPORT NUMBER

11. SUPPLEMENTARY NOTES

Prepared for Publication in Analytical Chemistry

12a. DISTRIBUTION AVAILABILITY STATEMENT

Unclassified

12b. DISTRIBUTION CODE

13. ABSTRACT *(Maximum 200 words)*

Construction and characterization of platinum and gold electrodes with total structural diameters of 1-2 μm is described. These small voltammetric probes have been constructed by direct electroreduction of noble metals onto the tips of etched carbon fiber microdisk electrodes. Voltammetry, electron microscopy, energy-dispersive x-ray analysis, and pulsed amperometric detection have been used to characterize these electrodes. Dopamine concentrations have been determined over a range of 10^{-4} to 10^{-3} M in the biological buffer system which contains 25 mM glucose, a compound known to adsorb strongly to electrodes. Amperometric monitoring at a constant potential with these small results in signal dacay of 20% to 40% in a ten minute experiment. Pulsed amperometric detection minimizes electrode fouling, resulting in 5% or less signal decay over the same ten minute period.

14. SUBJECT TERMS

gold electrodes, voltammetry, electron microscopy, energy dispersive x-ray analysis, pulsed amperometric detection

15. NUMBER OF PAGES

32

16. PRICE CODE

17. SECURITY CLASSIFICATION OF REPORT	18. SECURITY CLASSIFICATION OF THIS PAGE	19. SECURITY CLASSIFICATION OF ABSTRACT	20. LIMITATION OF ABSTRA
unclassified	unclassified	unclassified	

Characterization of Small Noble Metal Microelectrodes by Voltammetry and Energy Dispersive X-ray Analysis

Timothy G. Strein and Andrew G. Ewing*
Penn State University
152 Davey Lab
University Park, PA 16801

* Author to whom correspondence should be addressed

UPCOMING RESEARCH

Ultrasmall platinum and gold electrodes have been characterized with voltammetry, scanning electron microscopy, and energy dispersive X-ray analysis, and have been used in conjunction with pulsed amperometric detection to quantitatively monitor dopamine concentrations in the presence of glucose.

ABSTRACT

Construction and characterization of platinum and gold electrodes with total structural diameters of 1-2 μm is described. These small voltammetric probes have been constructed by direct electroreduction of noble metals onto the tips of etched carbon fiber microdisk electrodes. Voltammetry, electron microscopy, energy-dispersive x-ray analysis, and pulsed amperometric detection have been used to characterize these electrodes. Dopamine concentrations have been determined over a range of 10^{-4} to 10^{-3} M in a biological buffer system which contains 25 mM glucose, a compound known to adsorb strongly to electrodes. Amperometric monitoring at a constant potential with these small results in signal decay of 20% to 40% in a ten minute experiment. Pulsed amperometric detection minimizes electrode fouling, resulting in 5% or less signal decay over the same ten minute period.

INTRODUCTION

Ultrasmall voltammetric electrodes have found wide utility[1-3] for determination of fast electron-transfer kinetics,[4] for electrochemical microscopy,[5,6] and for the determination of electroactive species in complex biological environments.[7-10] A primary goal in our laboratories is to measure neurotransmitter dynamics in isolated microenvironments in order to better understand the complex process of neurotransmission. Working toward this goal, carbon electrodes have been used to examine dopamine dynamics in and immediately near single neurons of the pond snail *Planorbis corneus*.[11-13] In addition, attempts are presently underway to investigate smaller, human nerve cells grown in tissue culture. These cells are in the range of 10-40 μm in diameter, with synaptic contact regions clearly in the sub-micron regime.

Experiments designed to measure neurotransmitters at a single, isolated synapse have thus far proven very difficult for two primary reasons. First, the experiments require electrodes of suitably small diameter in both electroactive area and in total structural diameter to allow viewing of the microscopic manipulation of the probe into the extremely small area of interest. Second, the cultured neurons require a physiological buffer system which contains several chemical species that strongly adsorb to and foul electrode surfaces. We have recently reported a scheme to make carbon electrodes with total diameters in the sub-micron regime to eliminate the former problem.[14] However, electrode fouling remains a serious limitation in the measurements thus far obtained using the carbon probes.

Noble metal electrodes are useful for measurements in complex media where pulse techniques can be used to clean the electrode surface.[15-22] Conventional methods of cleaning electrode structures to obtain consistent electrochemical response usually include physical polishing of the electrode surface. Polishing at these structurally small probes has proven difficult, often resulting in a broken electrode tip. Consequently, other methods of obtaining a consistent electrochemical response without physical polishing of the electrode surface have been investigated. One method, pulsed amperometric detection (PAD) has been the subject of many publications over the past decade.[15-24] This method, which provides a means of obtaining a predictable, renewable electrode surface without polishing, consists of a series of potential pulses. First, a large anodic pulse results in the desorption of surface-bound species and causes a thin layer of oxide to be formed at the electrode surface. Second, a cathodic pulse causes the dissolution of

the oxide film and reactivates the electrode surface. The potential is then stepped to a value at which the detection occurs. By carefully choosing these three potentials and the time that each is applied, a large number of different detection scenarios can be achieved.

Extremely small noble metal electrodes can be constructed either by imbedding wires into small insulators[4,25], or by electrodepositing metal onto a small carbon electrode.[26-28] The mechanism of noble metal deposition onto small carbon electrodes has been investigated and apparently, the adhesion of the metal to the carbon surface is quite strong.[26] Applying this technology to yet smaller probe tips should allow the use of PAD, which does not work with carbon electrodes, to determine neurotransmitters in ultrasmall environments while minimizing the difficulties of diminishing response due to electrode fouling.

Ultrasmall carbon, platinum, and gold electrodes can be analyzed using Scanning electron microscopy (SEM) and energy-dispersive x-ray analysis (EDAX) to visually and chemically characterize the electrode tips. SEM along with EDAX is a powerful tool for studying electrodeposited material at extremely small electrode surfaces.[29-33] In addition to visualizing structure with electron microscopy, energy dispersive x-ray analysis allows element maps of the sample with identification of, and in some cases quantitation of, each element present in the sample. Clearly, this technique offers a powerful means to analyze small deposits of noble metal on the extreme tips of microelectrodes. In EDAX, atoms are electronically exited by the high energy electron beam in the scanning electron microscope, resulting in a core level electron hole in a sample atom. Characteristic X-ray emission lines corresponding to the energy loss when an outer-shell electrons fills a core hole are detected providing identification of the element(s) in the sample. Using this technique, we have qualitatively determined the presence of, and empirically determined the amount of platinum or gold at the extreme tips of the ultrasmall electrodes reported here.

This paper describes the construction and characterization of electrodes that can be used to minimize fouling in complex media. The electrodes described here are constructed by electrodepositing either platinum or gold onto the end of extremely small carbon disk electrodes and are then characterized by SEM and EDAX. These noble metal-based electrodes of suitably small size for neuronal microanalysis have been employed with pulsed amperometric detection (PAD) to minimize electrode fouling in a N-2-hydroxyethylpiperazine-N'-2-ethanesulfonic acid (HEPES) biological buffer system at physiological pH.

EXPERIMENTAL SECTION

1. Electrode Construction: Ultrasmall carbon disk electrodes were prepared as described previously.[14] Each carbon fiber, originally 11 μm in diameter, was etched in an intense methane/oxygen flame. This flame-etching procedure results in conical tips with tip diameters of approximately 100 nm.[14] The carbon fibers were then coated with an insulating copolymer film of phenol and 2-allylphenol, and the tip was cleaved with a scalpel blade to expose the carbon electrode surface. Noble metal electrode surfaces were constructed by direct electroreduction of noble metal cation onto the small carbon surface. Platinum deposition was accomplished by applying -0.25 V vs a sodium saturated calomel reference electrode (SSCE) to the electrode while the tip was immersed in 1 mM H_2PtCl_6 and 0.5 M H_2SO_4. Gold deposition was accomplished by holding the electrode at 0.00 V vs SSCE in 1 mM $AuCl_3$ and 0.5 M H_2SO_4. Deposition times were limited to 5 to 10 s to avoid large deposits of metal, thus limiting the amount of charging current in subsequent experiments. Each noble metal-coated electrode was tested for characteristic oxygen surface chemistry by scanning from 0.0 to 1.65 V vs SSCE in 0.5 M H_2SO_4 prior to use.

2. Chemicals and Solutions. A. Chemicals. Dopamine hydrochloride, α-d-glucose, magnesium chloride hexahydrate, and HEPES were obtained from Sigma Chemical Company, St. Louis, MO. Sodium phosphate, dibasic heptahydrate as well as sodium phosphate monobasic monohydrate, were obtained from J. T. Baker Inc., Phillipsburg, NJ, and calcium chloride dihydrate was obtained from Aldrich Chemical Company, Inc., Milwaukee, WI. All chemicals were reagent grade and used as received without further purification.

B. Noble Metal Deposition Solutions. Stock solutions of 0.01 M H_2PtCl_6 were prepared by dissolving 1.4 μm Pt powder (Johnson Matthey Inc., Seabrook, NH). in aqua regia. Gold deposition solutions were prepared from stock 0.01 M $AuCl_3$ made by the dissolution of 20 mesh gold powder (Johnson Matthey Inc., Seabrook, NH) in aqua regia.

C. Analysis Solutions. Buffer solutions used in this work were 0.05 M sodium phosphate, adjusted to a pH of 7.0 with sodium hydroxide, or 10 mM HEPES, 140 mM NaCl, 5 mM KCl, 25 mM glucose, and 2 mM $CaCl_2$ adjusted to a pH of 7.4.

3. Electrode Mounting and Preparation for SEM/EDAX. Electrode tips were mounted onto carbon SEM stubs (Electron Microscopy Sciences, Fort Washington, PA) which were filed down to a 45º angle on one side. The shaft of the electrode was held onto the slanted portion of the stub with electrical conducting carbon double-sided sticky tape (Electron Microscopy Sciences) such that the tip of the electrode rested just above the top of the stub. To ensure electrical conduction, the samples were then sputter-coated with carbon prior to analysis with the scanning electron microscope apparatus. The stubs were inserted onto the stage with the electrode tips pointed away from the detector. The stage was subsequently tilted 30º to obtain end-on imaging of the electrode tips without image distortion.

4. Equipment and Software. A. Electrochemistry. All electrochemical experiments were carried out in a copper-mesh faraday cage using an Ensman Instruments EI-400 (Ensman Scientific, Bloomington, IN) potentiostat in the 2-electrode mode. Computer-acquired data collection was accomplished with a Labmaster interface (Scientific Solutions, Inc., Solon, OH), and an IBM personal computer. A locally written software program was used to apply the potential waveform and to collect and plot the data.

B. Scanning Electron Microscopy and Energy-dispersive X-ray Analysis
Electron microscopy was carried out with a Jeol 5400 (Jeol, Peabody, MA) scanning electron microscope with a 20-30 kV accelerating voltage. EDAX data were collected with a lithium drifted silicon detector which is not a light element detector, for a duration of 100 s. X-ray data analysis was facilitated by use of the Integrated Microanalyzer for Imaging and X-ray Analysis (IMIX) software package and a Sun Sparc workstation. Both the detector and the software were purchased from Princeton Gamma Tech, Princeton, NJ.

RESULTS AND DISCUSSION

I. Electrode Construction and Characterization. A schematic of the noble metal electrodes described in this paper is shown in Figure 1. The core of the electrode is an extremely fine carbon fiber with the noble metal electrode surface at the tip of the fiber. These electrodes are constructed by etching the tip of a carbon fiber in a methane-oxygen flame and insulating all but the tip with a thin phenol-allylphenol copolymer film.[14] Electrodes with total structural diameters as small as 400 nm have been constructed using this procedure. To construct platinum microelectrodes, the small

carbon tip is electroplated with platinum at -0.250 V vs SSCE in 1 mM H_2PtCl_6. At this potential, platinum is irreversibly deposited as described by the following two step sequence:

$$Pt^{4+} + 2e^- \text{---> } Pt^{2+}$$
$$Pt^{2+} + 2e^- \text{---> } Pt_{(m)}$$

The voltammetry observed at various stages of the electrode construction process for a platinum-coated electrode is shown in Figure 2. Figure 2a shows the voltammetric response of an insulated carbon fiber electrode to a 3 x 10^{-4} M dopamine solution. Figure 2b shows the response of the same electrode in the same solution following the removal of the insulating polymer from the tip. Figure 2c illustrates the characteristic platinum background voltammogram obtained after coating the electrode tip with platinum and scanning from 0.00 to 1.65 V vs SSCE in 0.5 M sulfuric acid. The general features of the voltammogram in Figure 2c are consistent with those obtained at platinum electrodes of conventional size.[26]

Gold-coated electrodes have been constructed in a similar fashion to platinum-coated electrodes. Electroreduction of Au^{3+} by potentiostating at 0.0 V vs SSCE in 1 mM AuCl occurs in a single step described by:

$$Au^{3+} + 3\,e^- \text{---> } Au_{(m)}$$

Voltammograms obtained in 3 x 10^{-4} M dopamine at a polymer insulated, and a freshly cleaved carbon electrode are shown in Figures 3a and b, respectively. A voltammogram in 0.5 M sulfuric acid with this electrode following the gold-coating process is shown in Figure 3c. The voltammetric features observed in Figure 3c are similar to those reported at larger gold electrodes in sulfuric acid.[34] Both platinum and gold appear to be deposited onto the electrode surface spontaneously at the potentials applied, and give rise to the characteristic surface oxidation states of the two metals. Charging current contributions are higher with the platinum-coated tips than with the gold-coated tips, suggesting that the platinum is more porous in nature. For both platinum-coated and gold-coated electrodes, the electrochemical evidence points to good tip surface coverage and predictable background voltammetry.

Scanning electron micrographs of the electrodes corresponding to these voltammograms are shown in Figure 4. Figure 4a is an image of the platinum coated electrode, Figure 4b is an image of the gold coated tip, and Figure 4c is an image of an

uncoated carbon tip for comparison. In each case, the outer, smooth portion of the tip is the insulating polymer network, and the inner portion is the electroactive surface. The images shown in Figure 4 illustrate the morphological differences between the naked carbon tip (4c), and the tips which have had metal deposited onto the them (4a and 4b). The metals appear to have been deposited only at the electrode tip and not over the insulating polymer sheath.

To investigate the morphological evidence of the noble metal deposition onto the tip of the small electrodes, the tips shown in Figure 4 were further analyzed with EDAX. Figure 5 illustrates the utility of this technique for determining the deposition of noble metals onto extremely small carbon electrode tips. Figure 5a is an x-ray collection at the tip of the platinum coated electrode, Figure 5b is that from the gold plated electrode, and Figure 5c is obtained from the naked carbon electrode for comparison. The data shown here are x-ray collections obtained at a magnification of 10^5 centered at the tip of each electrode. The spectrum obtained at the platinum-tipped electrode (Figure 5a), illustrates two characteristic platinum lines: the M line, primarily Mα at 2.048 KeV, and the L line, primarily Lα at 9.441 KeV. The M line corresponds to the energy emitted from a platinum atom when an electron from the 4th electron shell (N) fills a hole in the in the 3rd electron shell (M), while the L line corresponds to an electron from the 3rd electron shell (M) filling a hole in the 2nd electron shell (L). Figure 5b shows the Mα (2.120 KeV) and Lα (9.712 KeV) lines for gold, and 5c shows the spectrum obtained from the carbon electrode tip, which shows no Mα or Lα lines. The relatively large peak at 1.486 KeV is due to the aluminum (Kα) mounting apparatus in the SEM column. The occurrence of platinum and gold x-ray emissions at the coated electrode tips and the absence of these emissions at the uncoated tip, supports the electrochemical and morphological data in that these structures have been successfully coated with the noble metals Pt and Au, respectively.

Figure 6 shows data monitoring the x-ray intensity at 9.441 KeV (Pt Lα) at the smaller platinum-coated electrode shown in Figure 4a as the beam spot has been rastered across the length of the tip region. The resulting line profile corresponds to the accumulated number of x-ray counts for a series of 10 scans with a dwell time of 30 ms at each point. The EDAX experiment strongly suggests that the tip of the coated electrode is platinized, whereas the sides are not.

Small clumps of what appear to be deposited material are often observed along the electrode shaft and away from tip. In order to determine if this material is the result of metal deposits (Pt or Au) on the insulation or at pin-holes in the insulation, x-ray data for both the electrode tip and the regions along the insulated shaft have been obtained.

X-ray emission spectra for this set of experiments is shown Figure 7. There are characteristic gold peaks in the spectra for points b, c, and d (Figures 7 B, C, and D), but there are no peaks indicating the presence of gold at point e (Figure 7E). These data indicate that the material deposited away from the tip is not gold. This material is likely an aberration of the polymer or a crystallized salt. The intensity of the peaks in Figures 7B and C, corresponding to the edge of the electrode are considerably higher than that in Figure 7D corresponding to point d in the center of the electrode. This result prompted the acquisition of a line profile across the tip monitoring the Au Lα intensity. The line profile monitored at 9.712 KeV across this electrode tip is superimposed on the image of the electrode tip in Figure 8. It is clear from these data that the gold is deposited on the entire tip, however it is deposited in significantly higher amounts at the edges. This can be attributed to the higher current density expected at the edge of disk-shaped microelectrodes, as a result of convergent edge diffusion of the Au^{3+} to the electrode surface.

II. Analysis with Noble Metal Microelectrodes: An eventual goal of these experiments is the measurement of the dynamics of neurotransmission at single synapses of human neuroblastoma cells. Unfortunately, the contents of the biological buffer system used to support the human neuroblastoma cells includes electrode-fouling components. Pulsed amperometry or pulsed amperometric detection (PAD) has been used to monitor the neurotransmitter dopamine in electrode-fouling buffer systems. The PAD waveform consists of an anodic potential pulse (+0.8 V vs SSCE for 50 ms) which desorbs surface adsorbates and oxidizes the metal surface, a cathodic pulse (-0.6 V vs SSCE for 150 ms) which reactivates the metallic surface, and a detection pulse (+0.7 V vs SSCE for 100 ms) for the quantitation of the analyte. The detection occurs in the last 16.7 ms of the 100 ms detection pulse, and is an average of 16 current samplings.

When the PAD waveform is employed to discriminate against adsorption of glucose oxidation products, the values of potential pulses in the PAD waveform were found to be especially important. The detection of glucose with this technique has been reported using 0.0 to +0.35 V vs SSCE as the detection potential.[31-33] This potential region is one in which the surface oxidation state of the noble metal surface apparently facilitates the adsorption and oxidation of glucose. The onset of this surface oxidation state can be as low as -0.4 V and continues to at least +0.35 V at gold surfaces in high pH solutions. In fact, the oxidation of glucose virtually ceases at higher potentials in alkaline media[30], apparently due to the formation of higher oxidation states of the gold surface. We have found this region to extend a bit further for analysis in neutral pH solutions, extending to approximately 0.6 V. For this reason, when attempting to discriminate

against glucose, a cathodic pulse of < -0.4 V, and anodic and detection pulses > +0.6 V should be employed. We have found +0.8 V vs SSCE for the anodic pulse, -0.6 V for the cathodic pulse, and a detection potential of +0.7 V to work well for monitoring dopamine in the presence of glucose. Both platinum and gold electrodes have been reactivated with this same potential pulse waveform.

The duration of the cathodic pulse is also critically important for proper quantitation. Empirically, we have found 150 ms to be adequate to reactivate electrodes with diameters of 1 - 11 μm . In one case, with an electrode tip of 1 μm, 25 ms at -0.6 was adequate to reactivate the gold-coated electrode. We anticipate that the use of smaller electrodes will allow shorter potential pulses to reactivate the electrode surface, allowing faster events to be monitored.

Figure 9 illustrates the utility of PAD for the quantitation and continuous monitoring of low levels of dopamine. The PAD waveform described has been applied to a gold-coated electrode for a period of ten min, over which the concentration of dopamine was increased three times. Each addition resulted in an increase in the oxidation current as monitored at +0.7 V vs SSCE. However, electrode fouling was clearly minimized by the PAD method.

An example of the difference between the response for PAD and amperometric detection at a constant potential is illustrated in Figure 10. A constant response for dopamine oxidation is obtained with PAD over the ten min period employed, whereas the oxidation current decays significantly for constant potential amperometry. The latter experiment shows an initial sharp drop, followed by a longer, more gradual decrease. The initial drop may represent charging current contributions, and as such this initial decay is not included in quantitation of electrode fouling. The constant-potential amperometric response shown in Figure 10b diminishes about 30% over 10 min. This large amount of electrode fouling makes quantitation of electroactive species difficult, and requires the use of both pre- and post-calibration procedures as well as an assumption of a linear decay in electrode response. No fouling is observed during the 10 min PAD experiment shown here (Figure 10a); however, some (6 out of 10) electrodes exhibit a small amount of fouling (2-10%) when the PAD experiment is run. The use of platinum and gold electrodes in conjunction with PAD under these conditions, results in a minimal amount of signal decay (inset in Figure 10), making calibration considerably easier. The PAD method, therefore provides a significant improvement for the consistent measurement of electroactive species at these electrodes.

Experiments similar to those described above and shown in Figure 10 were carried out for both platinum and gold electrodes in phosphate buffer systems as well as

in the biological HEPES buffer system containing 25 mM glucose. The results of several such experiments are summarized in Table I. Generally, the loss of electrode response is greater with Au-coated electrodes than with Pt-coated electrodes. In addition, electrode fouling seems to occur to a larger extent in the glucose-containing HEPES buffer relative to the non-glucose containing phosphate buffer system. However, a consistent, reliable signal with little electrode fouling is observed in all cases when the PAD potential waveform is used. In all of these experiments, the use of PAD in combination with ultrasmall noble metal electrodes should allow longer electrode life expectancy for experiments in complex biological media.

REFERENCES

1. Wightman, R. M. *Anal. Chem.* **1981**, *53*, 1125A-1134A.

2. Wightman, R. M.; Wipf, D. O. in *Electroanalytical Chemistry*, Bard, A. J. Ed., 1989, *15*, 267-353.

3. Fleischmann, M.; Pons, S.; Rolison, D. R.; Schmidt, P. P. *Ultramicroelectrodes*, Dalatech Sysytems: Morganton, N.C., 1987.

4. Penner, R. M.; Heben, M. J.; Longin, T. L.; Lewis, N. S. *Science* **1990**, *250*, 1118-1121.

5. Lee, C.; Miller, C. J.; Bard, A. J. *Anal. Chem.* **1991**, *63*, 78-83.

6. Bard, A. J.; Fan, F.-R. F.; Kwak, J. Lev. O. *Anal. Chem.* **1989**, *61*, 132-138.

7. Adams, R. N. *Anal. Chem.* **1976**, *48*, 1126A-1138A.

8. Wightman, R. M.; May, L. J.; Micheal, A. C. *Anal. Chem.* **1988**, *60*, 769A-779A.

9. Measurements of Neurotransmitter Release In Vivo; in Marsden, C. A. Ed.; *IBRO Handbook Series: Methods in Neurosciences*, vol. 6; J. Wiley: New York, 1984.

10. *Voltammetry in Neurosciences*; Justice, J. B., Ed.; Humara Press: Clifton, N.J., 1987.

11. Chien, J. B.; Saraceno, R. A.; Ewing, A. G. in *Redox Chemistry iand Interfacial Behavior of Biological Molecules*, ECS Symposium Series, Plenum Press: New York, 1988, 417-424.

12. Chien, J. B.; Wallingford, R. A.; Ewing, A. G. *J. of Neurochem.* **1990**, *54*, 633-638.

13. Lau, Y. Y.; Chien, J. B.; Wong, D. K. Y.; Ewing, A. G. *Electroanalysis*, **1991**, *3*, 87-95.

14. Strein, T. G.; Ewing A. G. *Anal. Chem.* **1992**, *64*, 1368-1373.

15. Johnson, D. C.; LaCourse, W. R. *Anal. Chem.* **1990**, *62*, 589A-597A.

16. Austin-Harrison, D. S.; Johnson, D. C. *Electroanalysis* **1989**, *1*, 189-197.

17. Auston, D. S.; Polta, J. A.; Polta, T. Z.; Tang, A. P.-C.; Cabelka, T. D.; Johnson, D. C. *J. Electroanal. Chem.* **1984**, *168*, 227-248.

18. Welch, L. E.; LaCourse, W. R.; Mead, D. A. Jr.; Johnson, D. C. *Anal. Chem.* **1989**, *61*, 555-559.

19. Polta, J. A.; Johnson, D. C. *J. Liquid Chrom.* **1983**, *6*, 1727-1743.

20. Larew, L. A.; Johnson, D. C. *J. Electroanal. Chem.* **1989**, *262*, 167-182.

21. Larew, L. A.; Johnson, D. C. *J. Electroanal. Chem.* **1989**, *264*, 131-147.

22. LaCourse, W. R.; Mead, D. A. Jr.; Johnson, D. C. *Anal. Chem.* **1990**, *62*, 220-224.

23. Andrews, R. W.; King, R. M. *Anal Chem.* **1990**, *62*, 2130-2134.25.

24. Roston, D. A.; Rhinebarger, R. R. *J. Liquid Chrom.* **1991**, *14*, 539-556.

25. Pendley, B. P.; Abruna, H. D. *Anal. Chem.*, **1990**, *62*, 782-784.

26. Georgolios, H; Jannakoudakis, D.; Karabinas, P. *J. Electroanal. Chem.* **1989**, *246*, 235-245.

27. Lau, Y. Y.; Wong, D. K. Y.; Ewing, A. G. *Microchem. J.* **1992** in press.

28. Lau, Y. Y.; Wong, D. K. Y.; Ewing, A. G. *Electroanalysis*, **1992**, in press.

29. Russ, J. C. *Fundamentals of Energy Dispersive X-Ray Analysis*, Butterworths & Co. Ltd: London, 1984.

30. Chong, N.-S.; Norton, M. L.; Anderson, J. L. *Anal. Chem.* **1992**, *64*, 1030-1033.

31. Chong, N.-S.; Anderson, J. L.; Norton, M. L. *J. Electrochem. Soc.*, **1989**, *136*, 1245-1246.

32. Bhattacharya, R. N.; Rajeshwar, K *J. Electrochem. Soc.* **1984**, *131*, 2032-2037.

33. Newbury, D. E.; Fiori, C. E.; Marinenko, R. B.; Myklebust, C. R.; Swyt, C. R.; Bright, D. S. *Anal. Chem.* **1990**, *62*, 1159A-1166A.

34. Rand, D. A. J.; Woods, R. J. *Electroanal. Chem.* **1972**, *35*, 209-218.

ACKNOWLEDGMENTS

This work was supported by the Office of Naval Research and the National Science Foundation. T.G.S. acknowledges support from an American Chemical Society Analytical Division Fellowship sponsored by the Proctor and Gamble Company. A.G.E. is the recipient of a Presidential Young Investigator Award from the National Science Foundation and is a Camille and Henry Dreyfus Teacher-Scholar. The authors wish to thank Rosemary Walsh for her assistance with the SEM and EDAX data presented this paper, and Professor Gouan Lou for writing the software to carry out the NAD/PAD experiments.

Table I. Average loss in response over a ten min period in two buffer systems for amperometric detection at a constant potential and PAD detection modes at noble metal-coated ultrasmall electrodes. Errors are expressed as standard deviations.

	% Fouling After Ten Min		
	PAD	**Normal Amperometric**	**n***
Platinum-coated			
Phosphate Buffer	1.8 ± 1.5	19 ± 15	6
HEPES Buffer	3.8 ± 3.0	22 ± 15	5
Gold-coated			
Phosphate Buffer	1.1 ± 1.9	40.4 ± 9.1	3
HEPES Buffer	6.4 ± 2.8	39 ± 15	3

* n = number of experimental trials

FIGURE CAPTIONS

Figure 1. Schematic of a noble metal microelectrode. The inset shows an end-on view of tip of the electrode tip. Key: W, nichrome wire; Ga, gallium; C, carbon fiber; P, insulating polymer film; M, electrodeposited noble metal.

Figure 2. Voltammograms obtained at different stages of the construction of a platinum electrode. (a) and (b) are voltammetric responses to a 3×10^{-4} M dopamine solution in phosphate buffer before (a), and after (b) the insulating polymer was removed from the tip. (c) shows the voltammogram obtained in 0.5 M H_2SO_4 after the carbon tip was coated with platinum. Scan rate: 100 mV/s. Scale: (a) 10 pA; (b) and (c), 100 pA.

Figure 3. Voltammograms obtained at different stages of the construction of a gold electrode. (a) and (b) are voltammetric responses to a 3×10^{-4} M dopamine solution in phosphate buffer before (a), and after (b) the insulating polymer was removed from the tip. (c) shows the voltammogram obtained in 0.5 M H_2SO_4 after the carbon tip was coated with gold. Scan rate: 100 mV/s. Scale: (a), 10 pA; (b) and (c), 100 pA.

Figure 4. Scanning electron micrographs of (a) the platinum coated electrode tip at which the voltammetry in Figure 2 was obtained, (b) the gold coated electrode tip at which the voltammetry in Figure 3 was obtained, and (c) a naked carbon electrode tip. Scale bar = 1 μm. Images are not as sharp as those presented earlier[14] because the samples were coated with carbon rather than gold. Carbon coating allows EDAX data to be collected, but sacrifices the image clarity for SEM.

Figure 5. EDAX data obtained at the electrode tips shown in Figure 4. (a) X-ray emission from the platinum coated tip, showing characteristic platinum peaks at 2.048 KeV and 9.441 KeV, (b) X-ray emission from the gold coated tip, showing characteristic peaks at 2.120 KeV and 9.712 KeV, and (c) x-ray emission from a naked carbon tip. All x-ray collections were performed at a magnification of 100,000 x centered on the electrode tip. Each spectrum is normalized to the largest peak, and the number of X-ray counts is shown in the upper right-hand corner of each spectrum.

Figure 6. A scanning electron micrograph and line profile showing the presence of Pt at the tip only. The line profile was monitored at 9.441 KeV, the Lα line for platinum. This is the same electrode shown in Figure 4(a).

Figure 7. SEM image and spectra obtained at several spots on a 10 μm diameter gold-coated electrode. The spectra B, C, D, and E correspond to points b, c, d and e, respectively.

Figure 8. Line profile across the tip of the gold-coated electrode shown in Figure 7 monitored at 9.712 KeV, the Lα line for gold.

Figure 9. The current response at a gold-coated electrode (ca. 1 μm dia.) using PAD upon three standard additions of dopamine to a phosphate buffer solution. Each addition consisted of 250 μL of 0.01 M dopamine into 25 mL of buffer solution, so each addition represents a change of approximately 0.1 mM dopamine. The solution was bubbled with N_2 for ca. 5 s following each addition to facilitate mixing.

Figure 10. Current response at a gold-coated electrode to 0.3 mM dopamine in phosphate buffer over a ten minute period. (a) Response using PAD, (b) response using normal amperometric detection. The experiment employed the same electrode and buffer system as above (ca 3.0×10^{-4} M dopamine). Inset: PAD experiment with enlarged current axis showing small, finite decay of response.

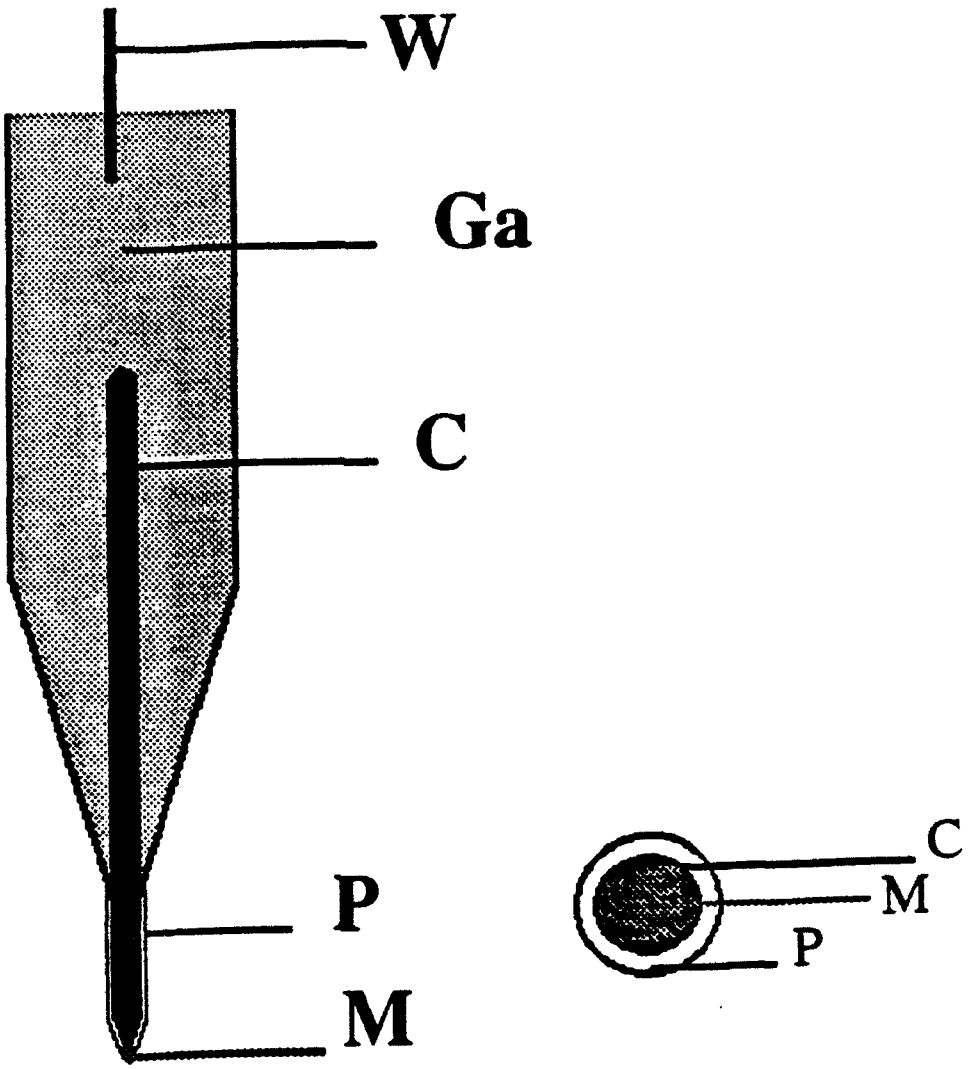
W
Ga
C
P
M
C
M
P

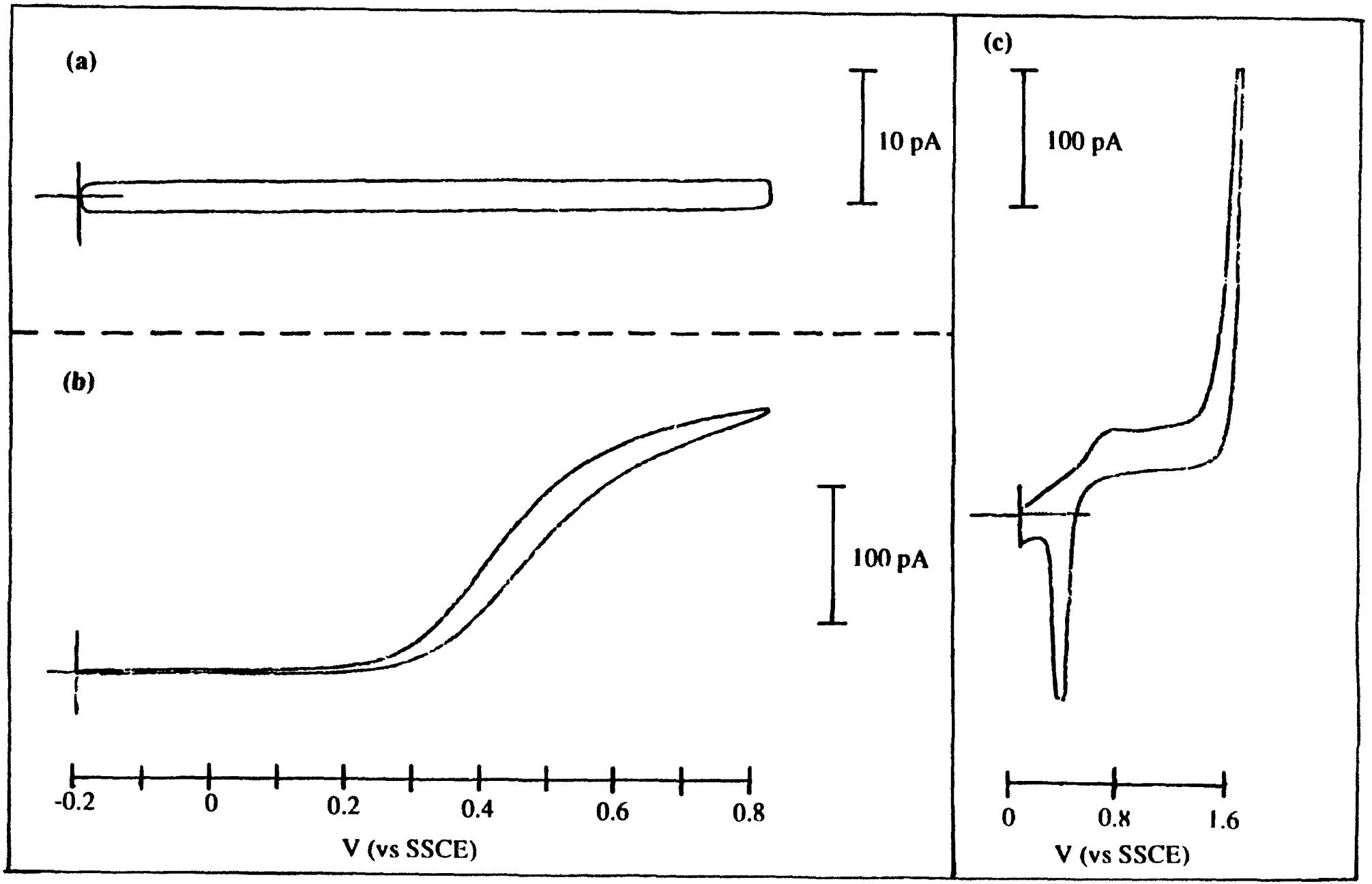
(a)
10 pA
(b)
100 pA
-0.2
0
0.2
0.4
0.6
0.8
V (vs SSCE)
(c)
100 pA
0
0.8
1.6
V (vs SSCE)

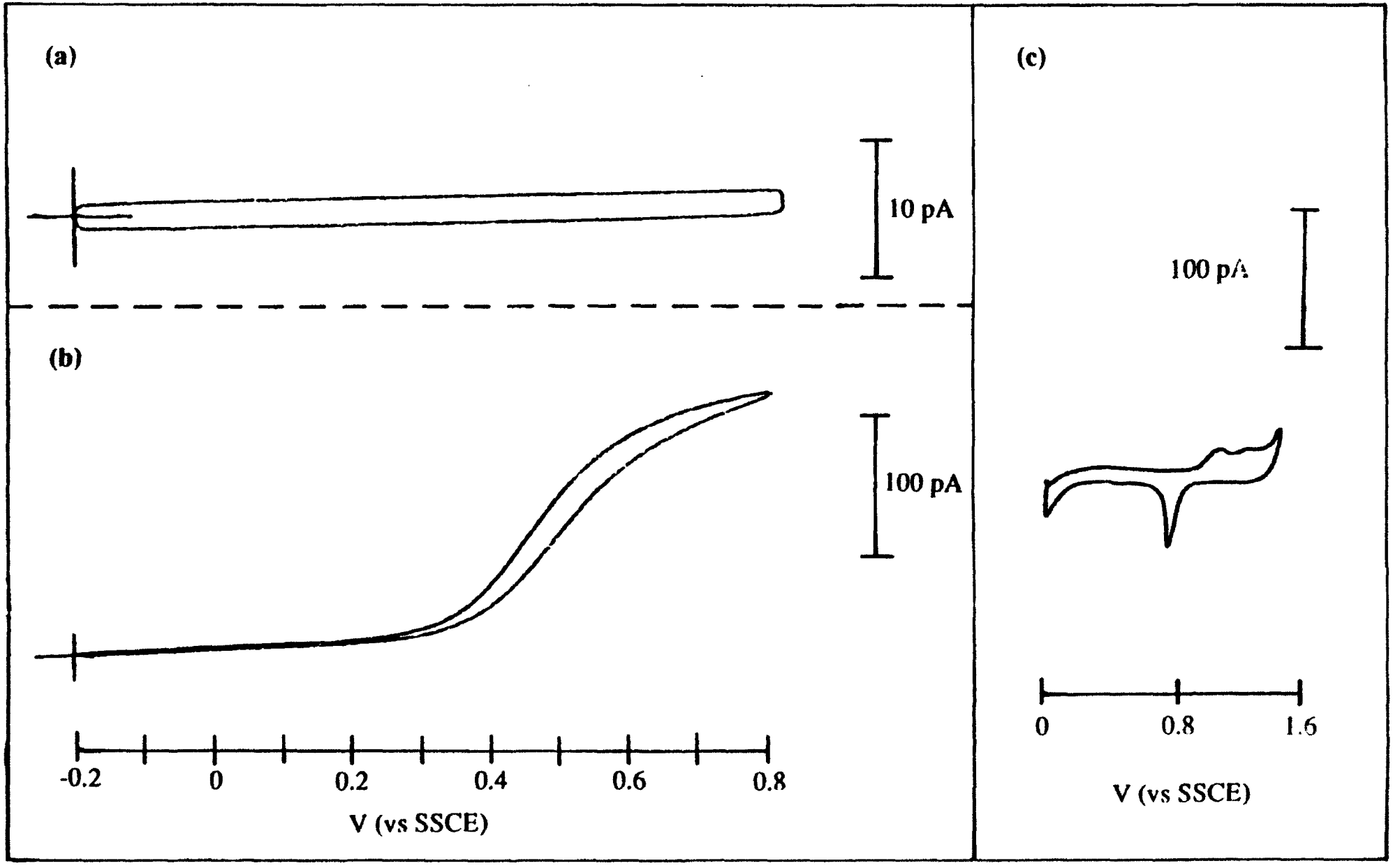
(a)
10 pA
(b)
100 pA
-0.2
0
0.2
0.4
0.6
0.8
V (vs SSCE)
(c)
100 pA
0
0.8
1.6
V (vs SSCE)

A

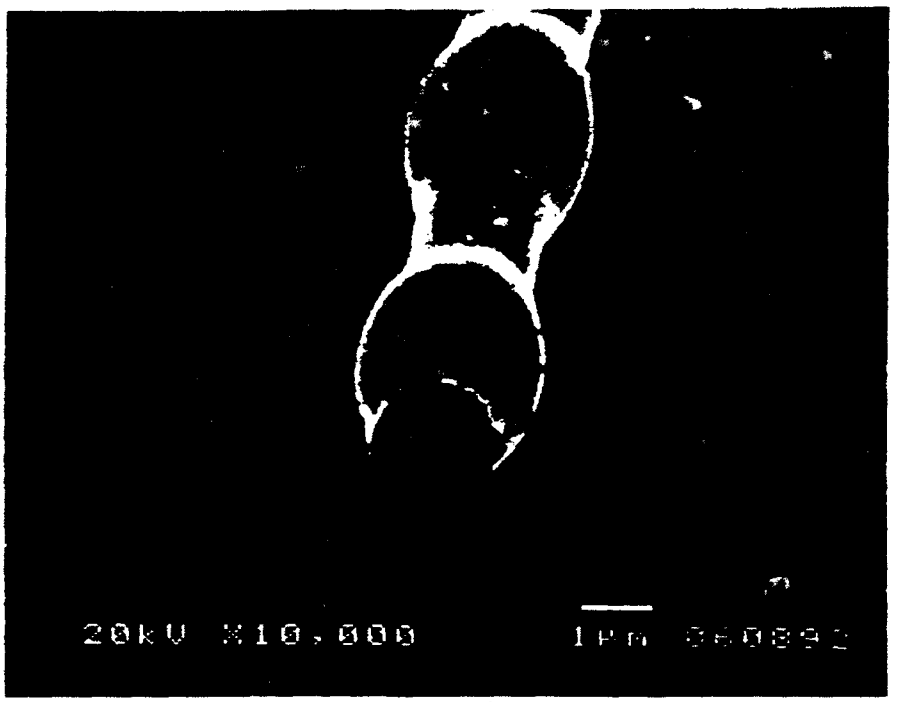

B

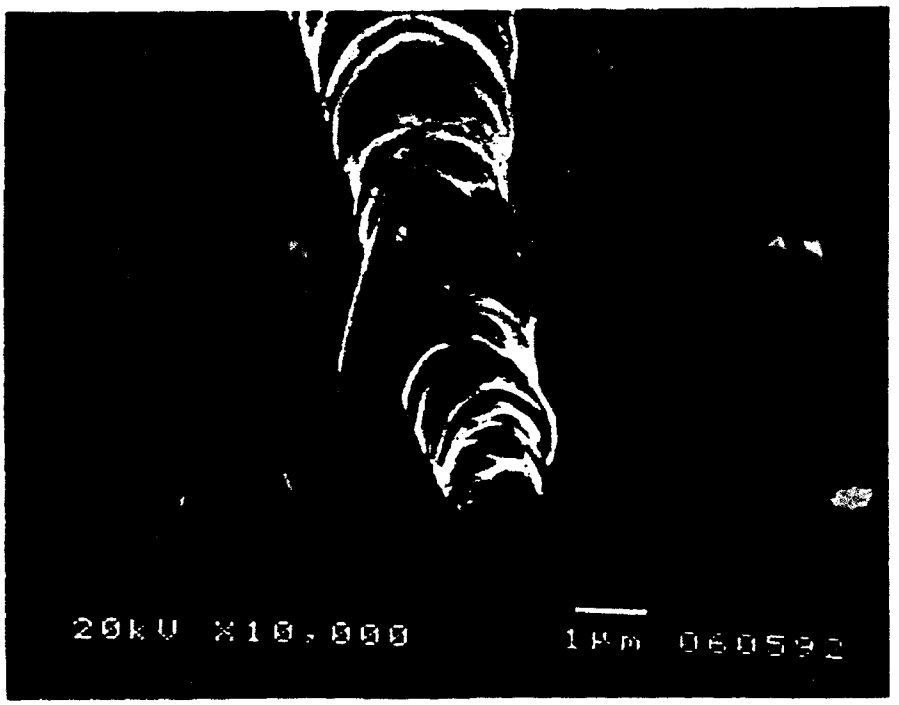

C

A

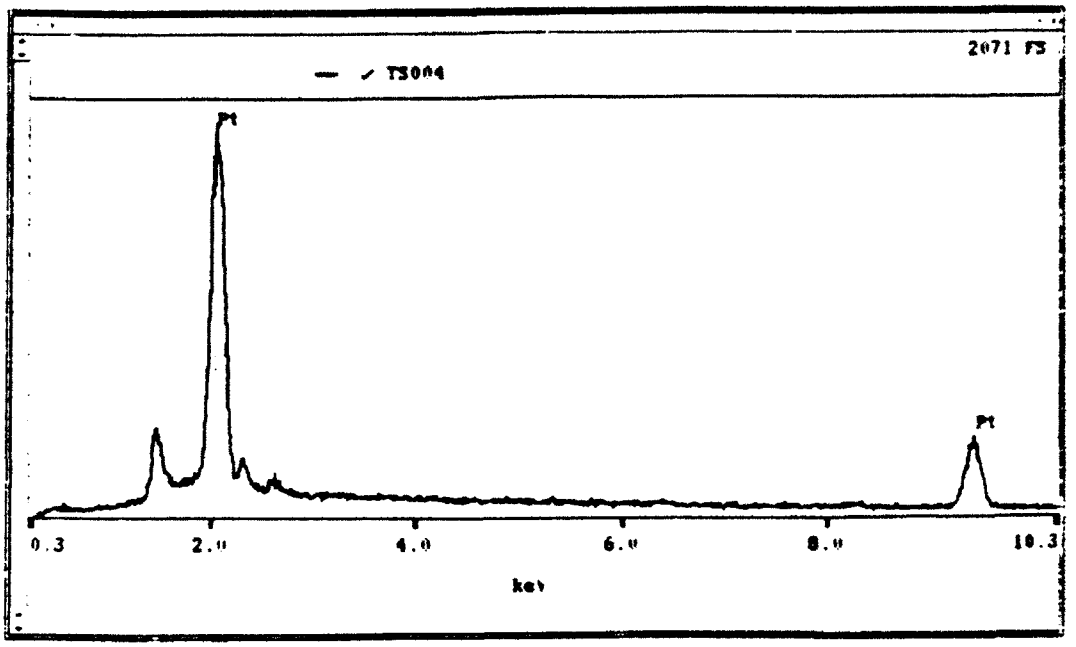
2071 FS
TS004
Pt
Pt
0.3
2.0
4.0
6.0
8.0
10.3
keV

B

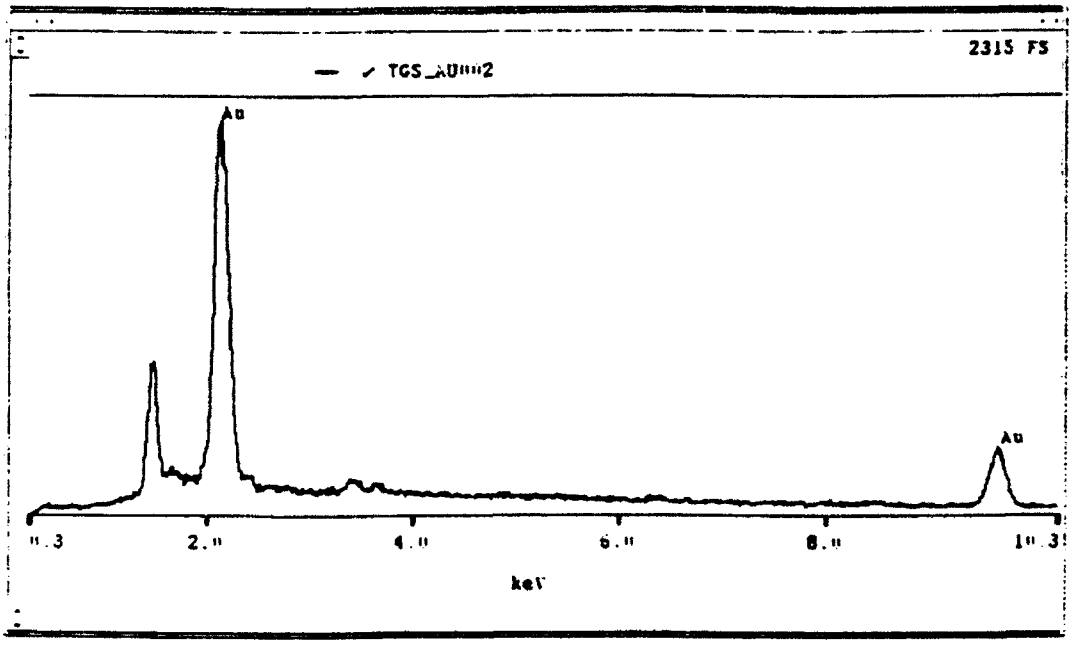
2315 FS
TGS_AU002
Au
Au
0.3
2.0
4.0
6.0
8.0
keV

C

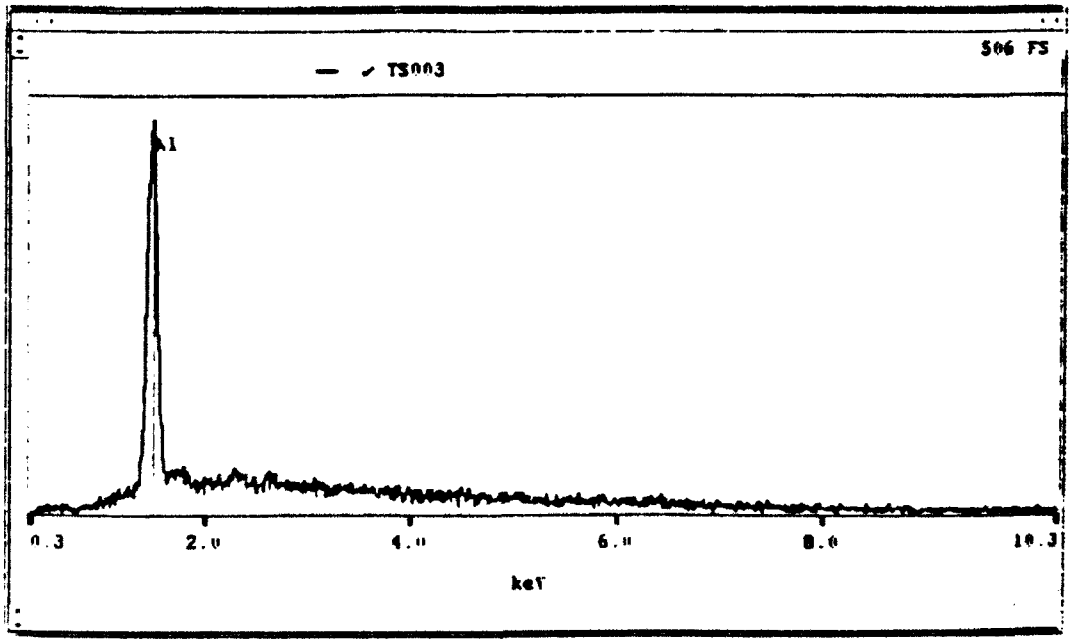
506 FS
TS003
Al
0.3
2.0
4.0
6.0
8.0
10.3
keV

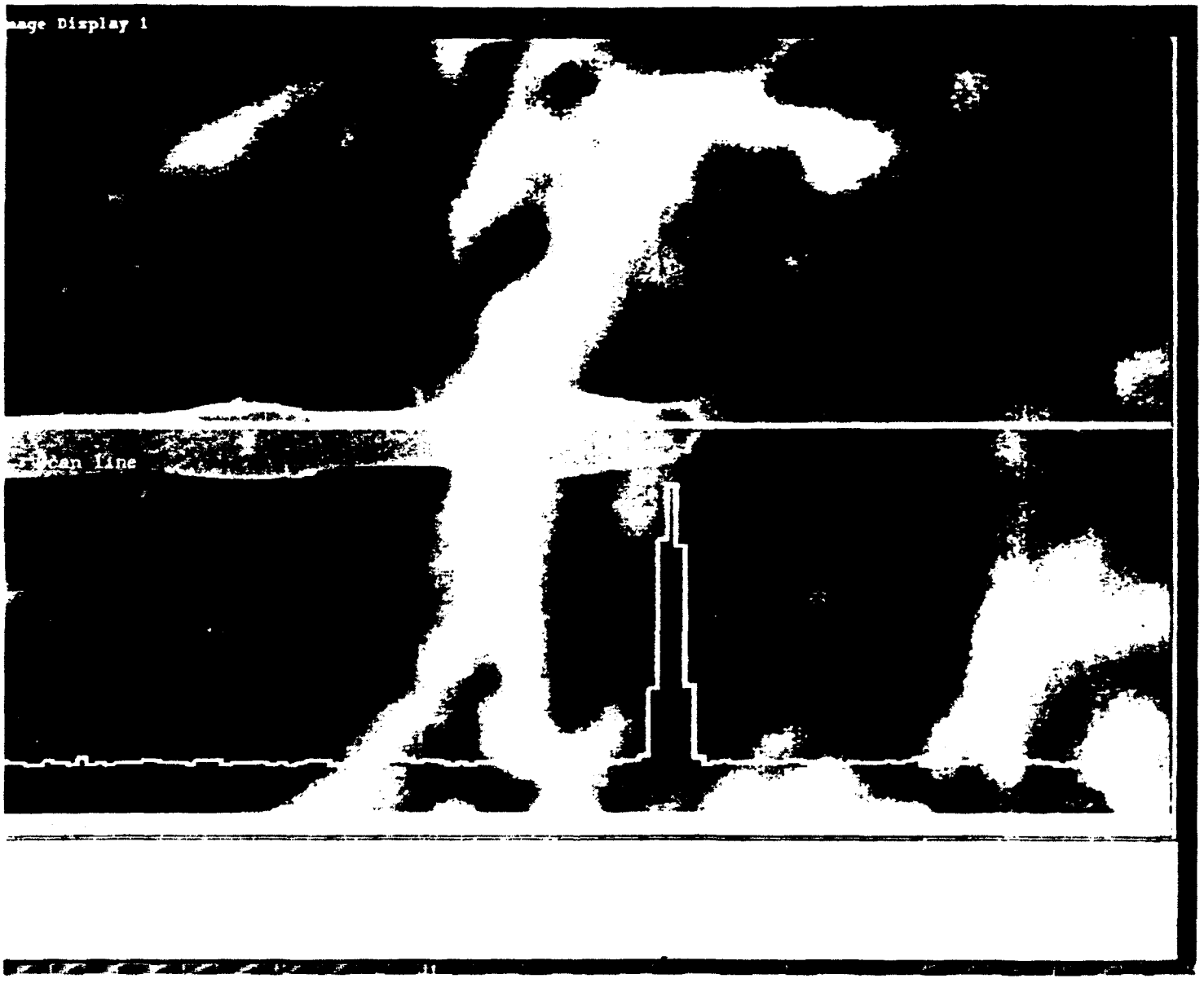
age Display 1
den line

A

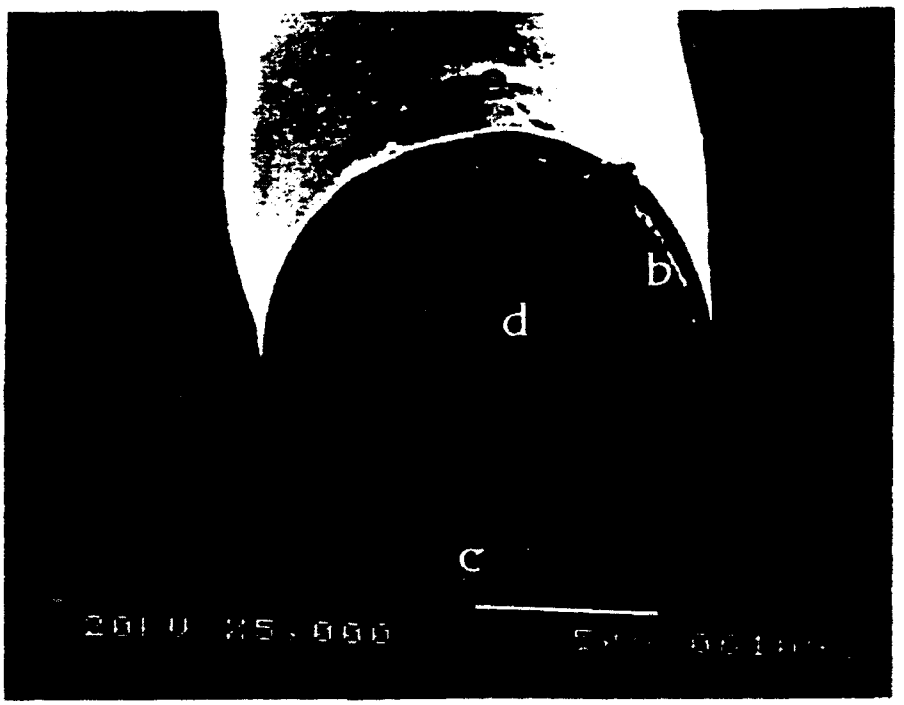

B

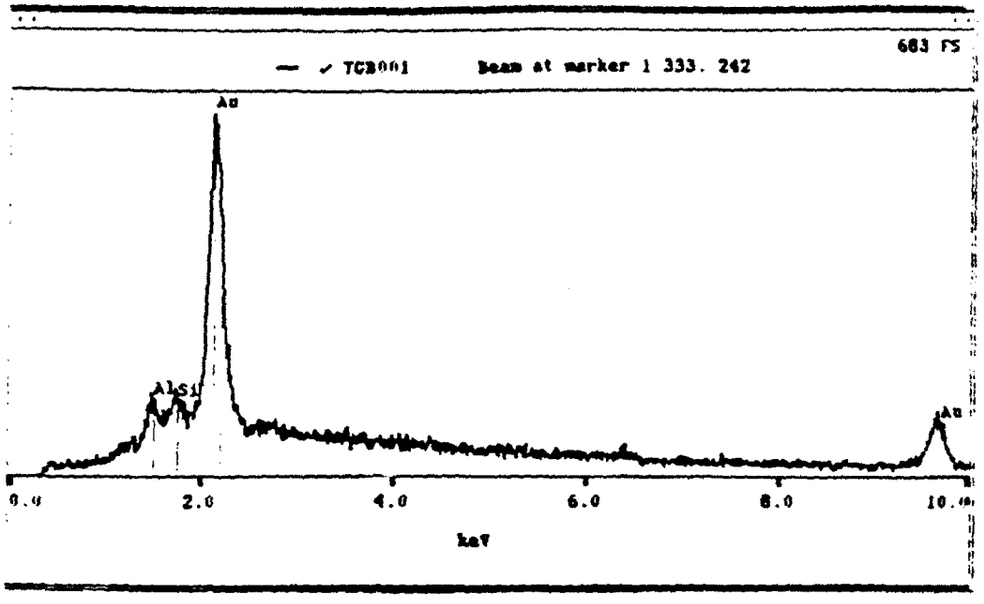
683 FS
✓ TCB001
Beam at marker 1 333. 242
Au
Al Si
Au
0.0
2.0
4.0
6.0
8.0
keV

C

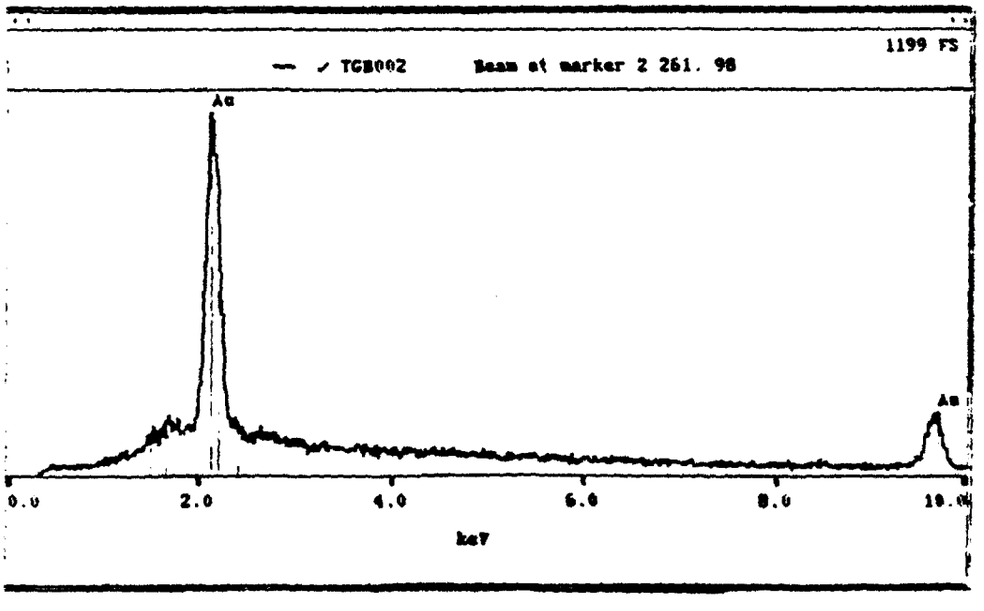
1199 FS
✓ TCB002
Beam at marker 2 261. 98
Au
Au
0.0
2.0
4.0
6.0
8.0
keV

D

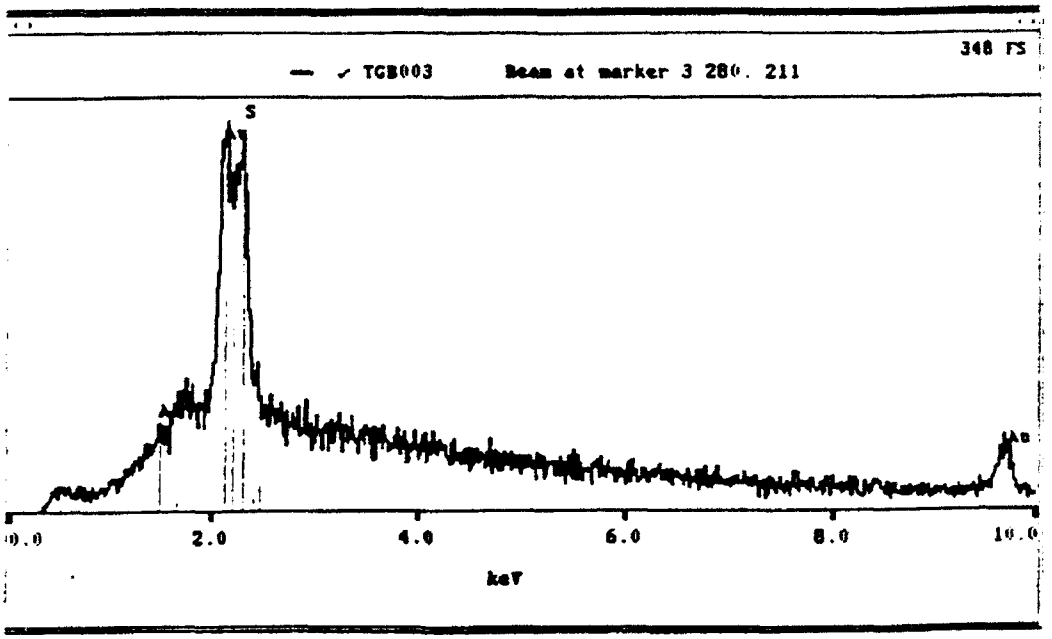
348 FS
— ✓ TGB003 Beam at marker 3 280. 211
S
2.0
4.0
6.0
8.0
keV

E

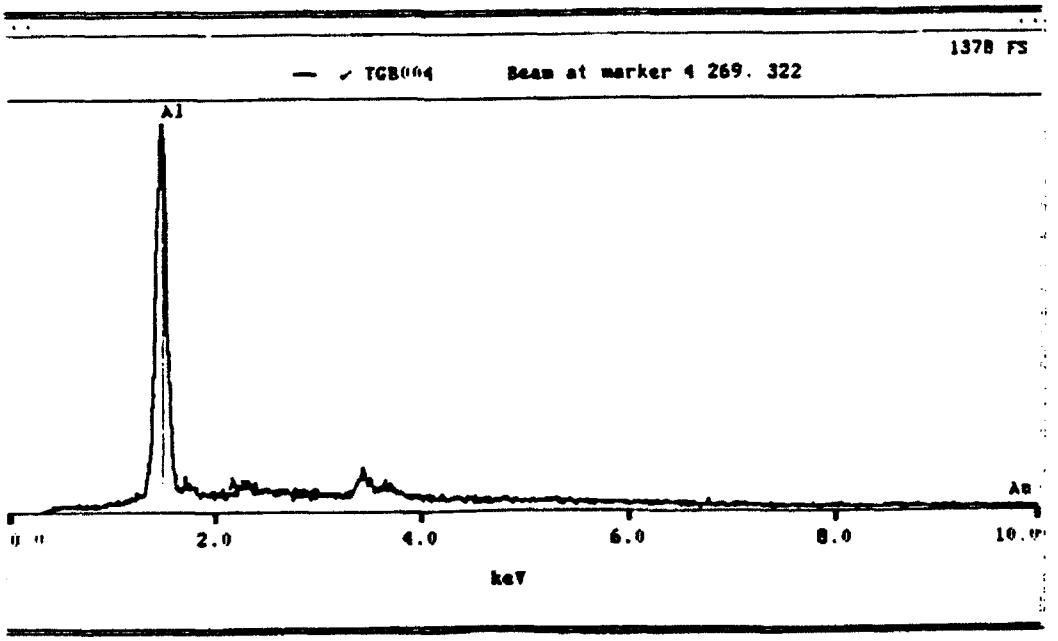
1378 FS
— ✓ TGB004 Beam at marker 4 269. 322
Al
2.0
4.0
6.0
8.0
keV

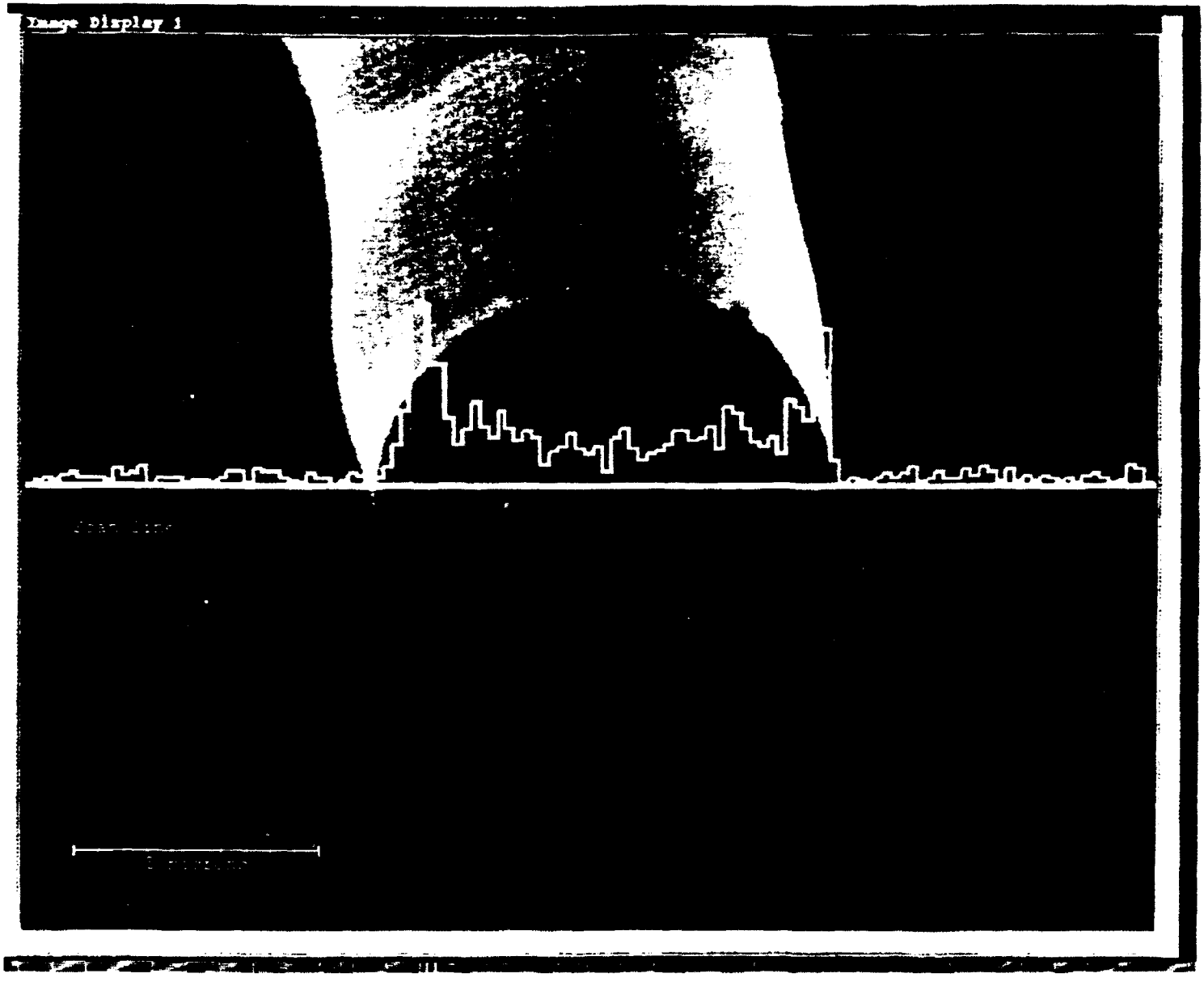
Image Display 1

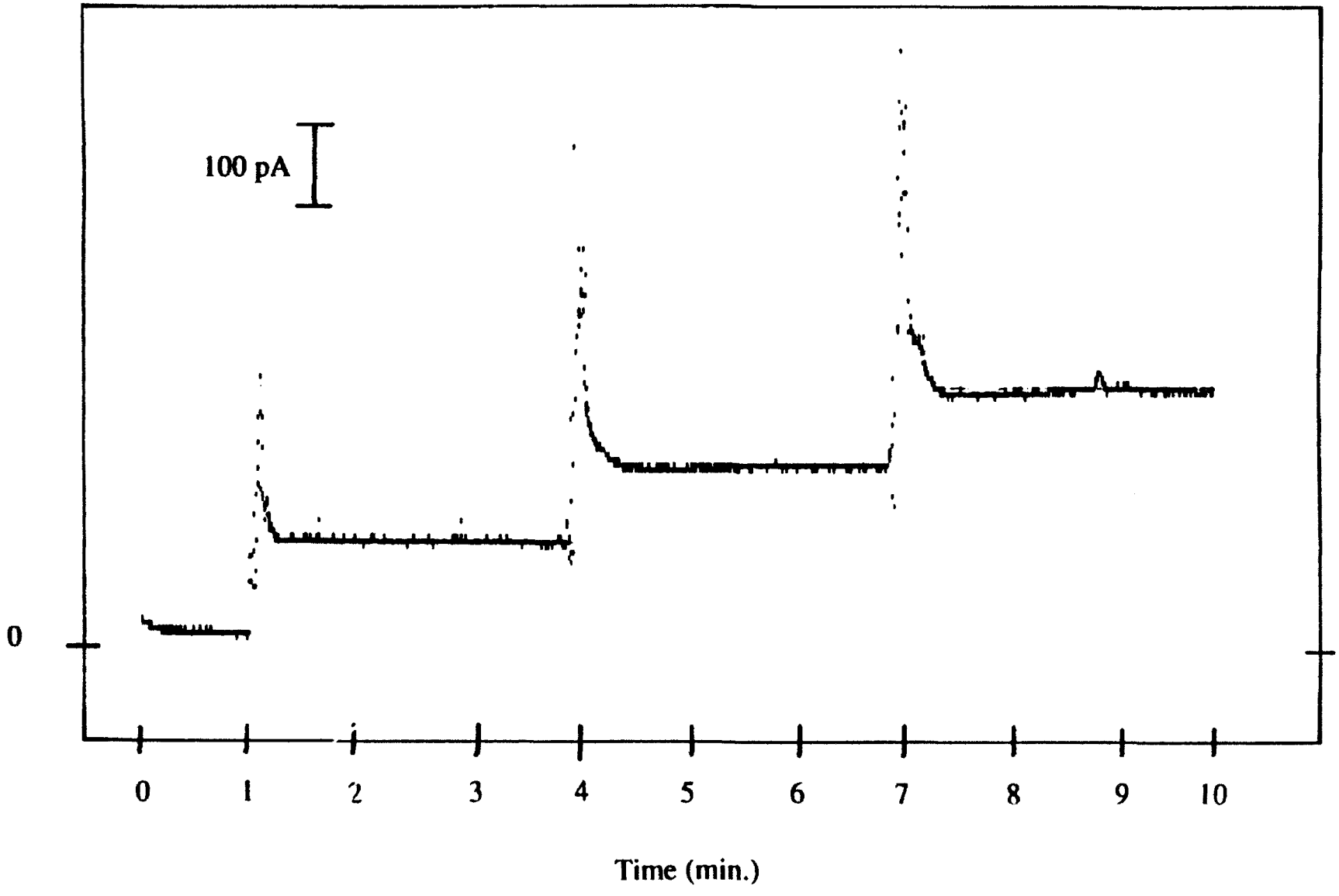
100 pA
0
0
1
2
3
4
5
6
7
8
9
10
Time (min.)

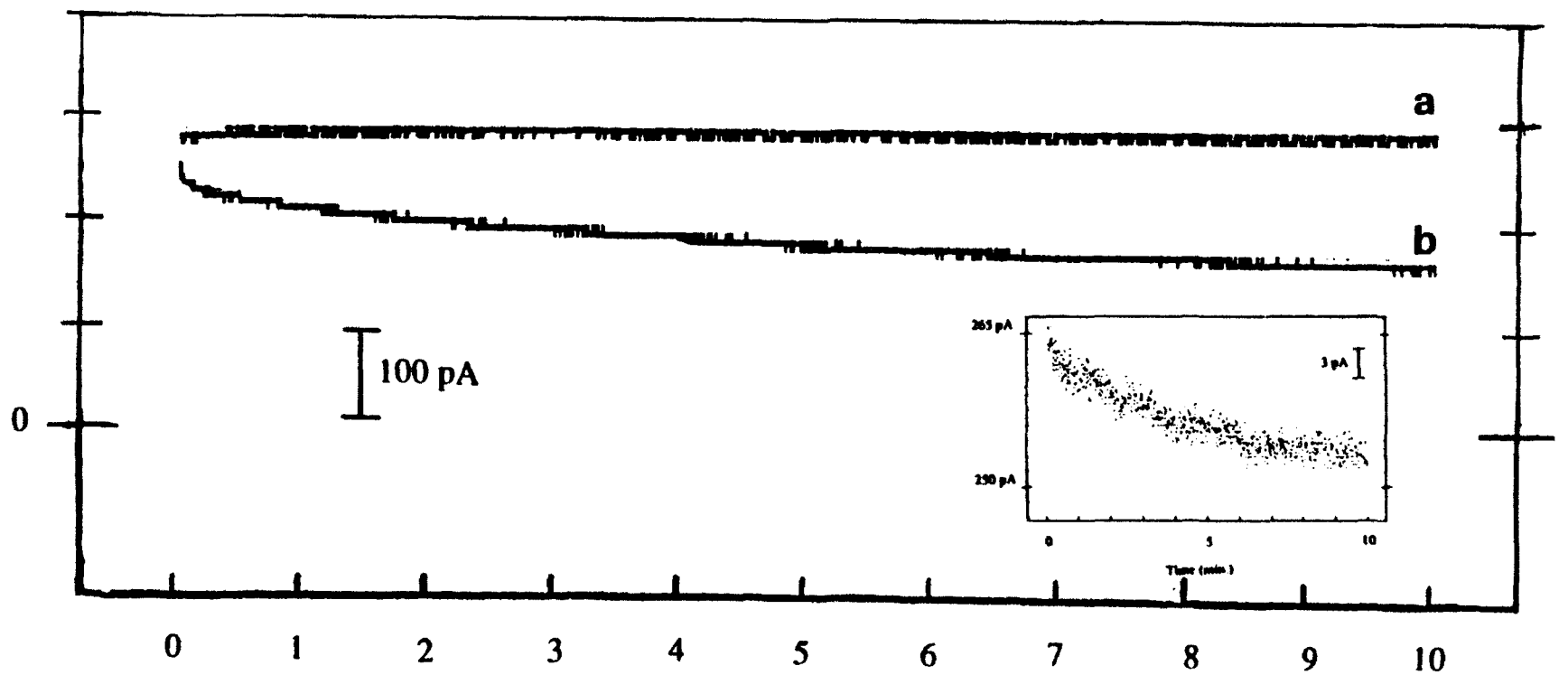
a
b
100 pA
0
0
1
2
3
4
5
6
7
8
9
10
Time (min.)